PNAS RESEARCH ARTICLE | ECOLOGY

Horseshoe bats foraging in the wild adjust sensing to separate prey echoes from background clutter

Yossi Yovel[a,b,1,2], Laura Stidsholt[c,1], Yotam Mimran[d], Mor Taub[a], Stefan Greif[a], Antoniya Hubancheva[e], Ivailo Borissov[a], Anthony J. Weiss[d], Annette Denzinger[f,1], and Hans-Ulrich Schnitzler[f,1]

Affiliations are included on p. 9.

Edited by Raghavendra Gadagkar, Indian Institute of Science, Bangalore, India; received September 11, 2025; accepted April 21, 2026

How animals handle immense incoming sensory information and regulate sensing is difficult to study under natural conditions. Using miniature GPS tags with microphones we monitored the sensing of freely foraging greater horseshoe bats. Bats stayed in acoustic contact with the environment and caught insects while commuting and in short flights from a perch. Bats adjusted their call frequency to maintain the highest-frequency echoes from background in a forward-directed, spatially limited sector at a constant maximal frequency. This Doppler-shift-compensation strategy guaranteed that echoes of insects flying in front of the bats were received at the sensitive center of their auditory fovea while masking background echoes were received at lower frequencies. Our results reveal an active sensing strategy allowing segregation of signals from background input under natural conditions.

Sensory acquisition | Echolocation | Doppler shift

Significance

Animals must constantly pick out vital signals from a flood of background noise, but how they do this in nature is poorly understood. Using tiny GPS-microphone tags on wild greater horseshoe bats, we found that these animals finely adjust the frequency of their sonar calls to keep echoes from flying insects centered in their most sensitive hearing range, while shifting background echoes away. This tuning allows bats to detect prey clearly even in cluttered environments such as forests and meadows. Our findings reveal a natural example of real-time sensory filtering, showing how brains can reduce noise by actively shaping the sensory input they receive—an insight relevant across species and sensory systems.

The detection of targets of interest and the segregation of desirable signals from background noise is arguably the most fundamental task of biological sensory systems. This task becomes especially challenging when moving through the real world, where animals are often swamped by sensory input, threatening to overload their sensory system and mask important target signals. Filtering essential signals from background can be performed at various levels of the system from the sensory periphery to the higher cortical regions. When possible, removing noise already at the acquisition level is ideal for detecting and evaluating desired signals because noise that is acquired by the system will probably be more difficult to remove at later stages (1, 2). One of the strategies applied by evolution for doing so is through active sensing—the process of adjusting sensory acquisition to optimize incoming input (3–6). In human vision, this active process is achieved by eye saccades which mediate the instantaneous acquisition of a very limited part of the visual scene at high resolution.

Active sensing is difficult to study under real-world conditions, mostly due to the difficulty of collecting information about both the sensory input and the sensory acquisition strategy in freely behaving animals. Here, we used a highly suitable model—an echolocator (7, 8)—which allowed us a unique opportunity to study auditory active sensing in freely foraging horseshoe bats under completely wild conditions.

The greater horseshoe bat, *Rhinolophus ferrumequinum* (Schreber, 1774), is an insectivorous bat that emits high duty cycle multiharmonic echolocation signals with a long constant frequency (CF) component, with the main amplitude in the second harmonic surrounded by frequency modulated (FM) components on both sides (Fig. 1*A*). The main function of the FM component is range estimation (9–12), however, we did not focus on it. The CF component which was the focus of this paper, is used by the bats to detect fluttering insects (13). In the laboratory, flying bats compensate for the Doppler shifts (DS) in echoes from targets straight ahead by lowering their emission frequency according to their flight speed, a strategy known as Doppler-shift-compensation (DSC, Fig. 1*B*). The bats lower their emission frequency so that the CF part of the echoes returning from large stationary targets ahead is kept constant with high accuracy at a frequency of 150 to 200 Hz above the resting frequency–the frequency emitted when the bat is at rest ($\mathbf{f_{rest}}$) (14, 15). These bats' specialized hearing system (16) is characterized by an auditory fovea, a highly expanded frequency representation on the basilar membrane of the cochlea with afferent projections to foveal centers that contain many sharply tuned neurons with the highest density at the 1 kHz wide central range of the fovea starting at $\mathbf{f_{rest}}$ (Fig. 1*C*) (for review see refs. 17 and 18).

Ensonification experiments with simulated CF signals have shown that echoes from fluttering insects contain a typical pattern of amplitude and frequency modulations which

Author contributions: Y.Y., L.S., and S.G. designed research; Y.Y., L.S., S.G., A.H., and I.B. performed research; Y.Y., L.S., M.T., A.D., and H.-U.S. contributed new reagents/analytic tools; Y.Y., L.S., Y.M., A.J.W., A.D., and H.-U.S. analyzed data; and Y.Y., A.D., and H.-U.S. wrote the paper.

The authors declare no competing interest.

This article is a PNAS Direct Submission.

[1]Y.Y., L.S., A.D., and H.-U.S. contributed equally to this work.

[2]To whom correspondence may be addressed. Email: yossiyovel@gmail.com.

This article contains supporting information online at https://www.pnas.org/lookup/suppl/doi:10.1073/pnas.2525520123/-/DCSupplemental.

Published June 22, 2026.

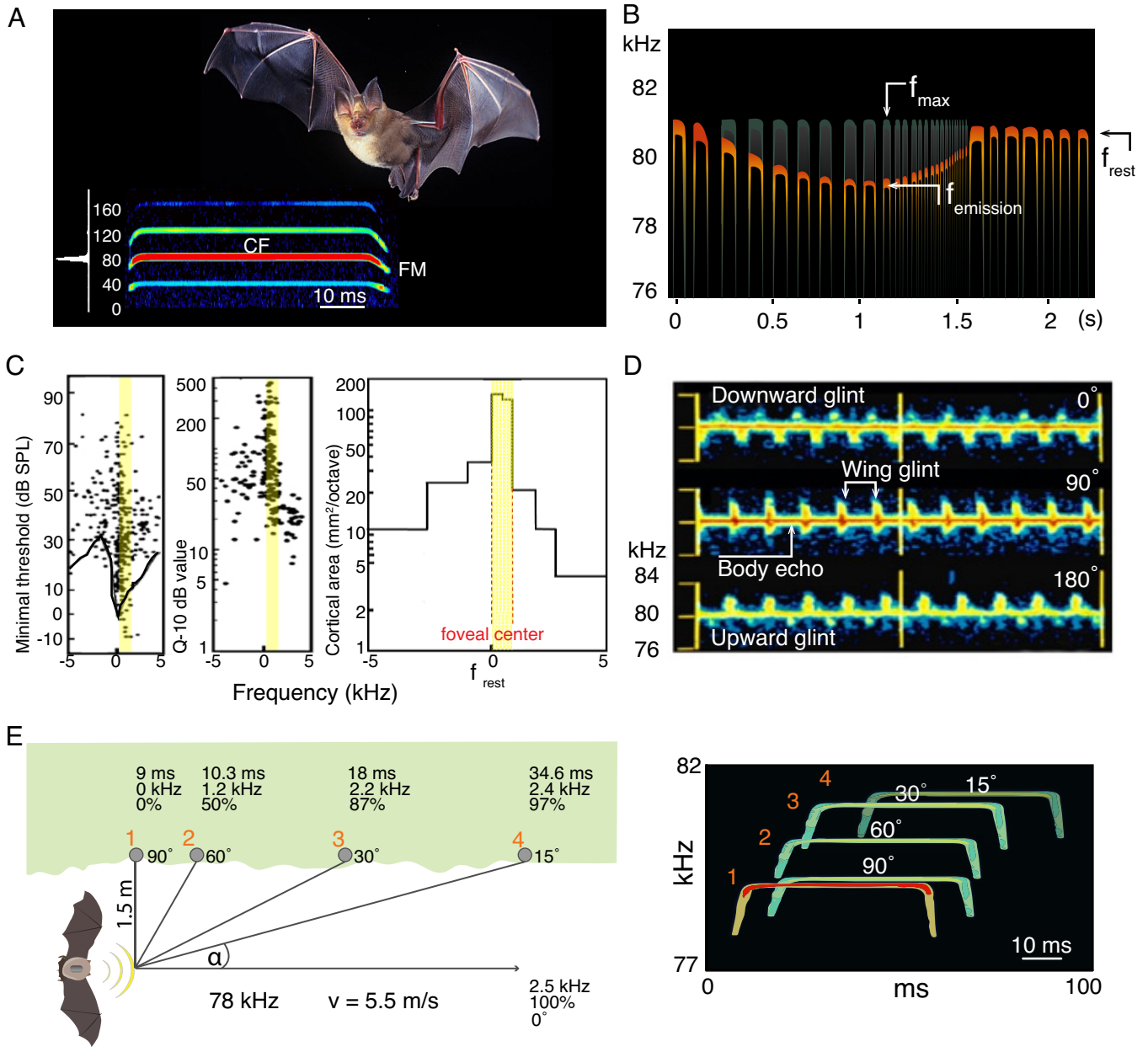

Fig. 1. The echolocation challenge of horseshoe bats. (*A*) The echolocation signal of the greater horseshoe bat. The multiharmonic signals (cyan, red, green, and blue) consist of a long component of constant frequency (CF), with the main amplitude around 80 kHz, which is preceded and followed by short frequency-modulated (FM) sweeps (FM-CF-FM signals). (*B*) Schematic Doppler shift compensation performed by bats flying in the laboratory from a starting point to a landing site. (*C*). The frequency representation of the auditory fovea is demonstrated here by the distribution of best frequencies of neurons in the auditory cortex. The most sensitive center of the fovea (marked in yellow) corresponds to a 1 kHz wide frequency range just above the resting frequency. It is characterized by single neurons with the lowest thresholds and by the highest sensitivity of the behavioral hearing curve (*Left*), by neurons with highest Q-10 dB values (*Middle*), and with the highest frequency expansion of the foveal system (*Right*) (measured by the cortical area per octave) (Credit line for *C*: adopted from ref. 19). Neurons in this area of the fovea are specialized to evaluate flutter information (20, 21). (*D*) The ensonification of a tethered fluttering marsh fly (Tipula oleracea) from different angles with a CF signal of 80 kHz produced short spectral glints created by DS generated when the moving wing was perpendicular to the impinging sound waves. The spectral glints point upward in insects flying away from the bat (180°) as the wings are moved backward in the instant of glint production. Downward glints are generated when the insects are flying toward the bat (0°) and double-sided glints are generated at 90°. The glint pattern also contains information on wing beat frequency and horseshoe bats have been shown to use this flutter information to evaluate prey characteristics in the lab (reviewed in ref. 17). (*E*) A greater horseshoe bat flying along vegetation receives echoes from environmental targets at different bearings and decreasing delays (*Left*). The DS depends on the relative speed vectors between the bat and the reflecting objects. It is 100% at a bearing angle (α) of 0° and decreases with the cosine of the bearing angle to 0% at 90°. A schematic spectrogram for this scenario with the emitted signal and the overlapping echoes the bat would receive (*Right*). The red signal represents the emitted signal while the green-yellow ones depict the echoes.

are caused by the insect's moving wings (13, 22). Especially prominent are short amplitude and frequency modulations (termed ***glints***) which are caused in the short instances when the insects' wings are perpendicular to the impinging sound waves. Psychophysical studies show that bats use this flutter information to discriminate between insect species and different aspect angles (23).

In stationary bats hanging at a perch, the carrier frequency of echoes returning from the body of the insect ($\mathbf{f}_{car}$) and the direction of the wideband spectral glints generated by their fluttering wings (upward or downward) depend on the relative speed vector of the insect. $\mathbf{f}_{car}$ of insects flying toward the bat is above $\mathbf{f}_{rest}$ and the glints point downward. In contrast, $\mathbf{f}_{car}$ of insects flying away is below $\mathbf{f}_{rest}$ and the glints point upward (Fig. 1*D*). Thus,

stationary bats searching for prey from a perch always have the big advantage that the glint pattern in prey echoes covers the most flutter sensitive center of their auditory fovea.

However, bats pursuing a fluttering insect on the wing have the problem that the speed vector between bat and prey does not only depend on the prey insect's relative speed vector toward or away from the bats alone but also on the bat's relative flight movement. The additionally induced DS are rather large, e.g., 2.5 kHz for echoes from straight ahead at a typical flight speed of 5.5 m/s. When searching for prey in flight near vegetation or near the ground, in the real-world, after each emitted signal, the bats will receive a series of many overlapping echoes from objects which differ in DS according to different bearing angles (i.e., the angle to the direction of flight—α) and in delays according to the different distances. Thus, multiple clutter echoes from background objects may overlap with the long echolocation signals and the insect echoes which increases the risk that echoes of the desired prey are masked by background clutter (Fig. 1*E*). Acoustic detection of insects near vegetation is thus a very difficult "signal from background" sensory task. DSC would provide a sensory advantage by enabling the detection of moving targets, such as live prey, amid complex and cluttered acoustic backgrounds. However, applying DSC in the real world is much more challenging than in the laboratory. It is currently unclear if and how bats compensate for DS when flying and foraging along or above vegetation while receiving many echoes from different directions.

Using miniature GPS and microphone tags mounted on free-flying bats in the field, we investigated how foraging greater horseshoe bats adapt their sensory acquisition for prey detection and clutter-noise rejection. Our microphones were sufficiently sensitive to record not only the emitted signals and the multiple echoes returning from background objects, but also the weaker echoes with carrier frequency and glints from fluttering prey during the final stages of the attack. This allowed us to study how bats adjust their emission frequency in response to the multiple Doppler-shifted target echoes they received. The GPS data revealed where the bats foraged and how fast they moved. We show how bats optimize sensory acquisition by tuning their emission frequencies such that the echoes from fluttering prey insects are focused within the center of their auditory fovea, which is specialized for flutter detection, while masking background echoes are received at lower frequencies, preventing interference with the higher-frequency prey echoes. With this strategy horseshoe bats actively segregate desirable signals which indicate fluttering prey from background echoes even in highly complex environments already at the peripheral acquisition level.

Results

Flight and Foraging Behavior. In total, we documented the behavior of nine bats (each for at least 4 h), three with both audio and GPS recordings, five with audio and acceleration recordings (no GPS) and one with GPS only. The bats commuted either along vertical background like vegetation or above horizontal planes like fields, meadows, or water surfaces to their individual main foraging areas (up to 40 km from their roost) where they foraged from perches (Fig. 2). During their commuting flights, the bats flew at an average speed of 5.5 ± 1.5 m/s. They hunted on-the-wing and paused for short periods of perch hunting.

The Capture of Fluttering Insects. The bats searched for prey on the wing while commuting to their main foraging areas as well as while hanging at a perch. Insect pursuits were indicated by a change from emitting single signals to an approach sequence with a higher signal-rate, which ended with a group of short signals, also known as a buzz (Fig. 3 *A* and *B*). We analyzed insect captures recorded from bats searching for prey on the wing (Fig. 3*A*) and from bats hunting from a perch (Fig. 3*B*). In our data, 77 ± 19% of the attacks on insects (mean ± SD, n = 5 bats) were performed while searching for prey on the wing, while 23% of the attacks were recorded during short sally flights performed after detecting prey from a perch.

In flying bats, the emitted signals overlapped with series of multiple echoes from near-by vegetation which differed in their DS and delays according to the different bearing angles and distances to the reflecting objects (Fig. 3 *A* and *B*). The flying bats lowered the frequency of their emitted signals so that the most upward Doppler shifted echoes were always kept constant at a maximal frequency ($\mathbf{f_{max}}$) of 320 ± 61 Hz (mean ± SD, n = 3 bats) above resting frequency ($\mathbf{f_{rest}}$, Fig. 3*C*). This strategy was used at all flight speeds when the bats sped up or slowed down during an attack as can be seen in the spectrograms (see gray arrows in Fig. 3 *A* and *B*). By lowering the emitted CF, bats adjusted both the echoes from the environment and the insect echoes in relation to the most sensitive area of their auditory fovea that spans over a 1 kHz range starting at $\mathbf{f_{rest}}$ (Fig. 1*C*, the area between the two horizontal red lines). Background echoes were kept below $\mathbf{f_{max}}$ so that the foveal flutter-sensitive frequency range above $\mathbf{f_{max}}$ was kept free of background echoes and available for detecting prey echoes.

All insect-echo sequences which were recorded during the final parts of the pursuit (Fig. 3 *A* and *B*) had upward glints, indicating that the bats were always approaching the insects from behind (Figs. 1*D* and 3). The carrier frequency ($\mathbf{f_{car}}$) of the echoes, which correspond to the weaker echo returning from the insect's body, was 300 to 500 Hz below $\mathbf{f_{rest}}$ (see orange rectangles in Fig. 3 *A* and *B*). The upward prey echo-glints were wideband and spread up to 3.1 kHz above the frequency of the weak body echo, thus covering the entire spectral range of the center of the auditory fovea (see green rectangles in Fig. 3 *A* and *B*). Our tags were not sensitive enough to record the insects' echoes at the instant of detection, therefore, we could not determine the angular orientation of the prey at those instances. Overall, the DSC strategy applied by the bats segregates background clutter echoes which remain below $\mathbf{f_{max}}$from the upward prey glints which arrive above $\mathbf{f_{max}}$and extend into the unmasked area of the flutter sensitive central auditory fovea.

Doppler Shift Compensation under Complex Natural Conditions. When flying near or above the vegetation, the bats flew at a distance of 1 to 2 m from the vegetation allowing them to maintain acoustic contact with the background. We could estimate this based on $\mathbf{f_{max}}$ echoes and the bearing angle (α) (Fig. 4 *A* and *B* and see *Materials and Methods*) and this was also confirmed by rare recorded zero-DS echoes which returned from the side vegetation 90° relative to the flight direction. The bats always received background echoes from multiple bearing angles, but not from straight ahead. The reconstruction of the acoustic scenes (Fig. 4 *A* and *B*) showed that the targets which produced $\mathbf{f_{max}}$ echoes with the largest DS had an average bearing angle of α = 23.2 ± 4.5° relative to the flight direction of the bats and distances of up to ~4 m from the bat (Fig. 4 *A* and *B*).

These echoes from around ~23^0 were fully compensated for (100% compensation re 23^0) and thus uncoupled from the flight-induced DS. Accordingly, all echoes from insects with bearing angles between 0^0 and 23^0, which have higher speed vectors and therefore higher DS, are undercompensated (by 8% at 0^0) whereas echoes from directions below have lower DS and are overcompensated. As the cosine changes slowly at small bearing angles, the sector in which the degree of compensation is still high

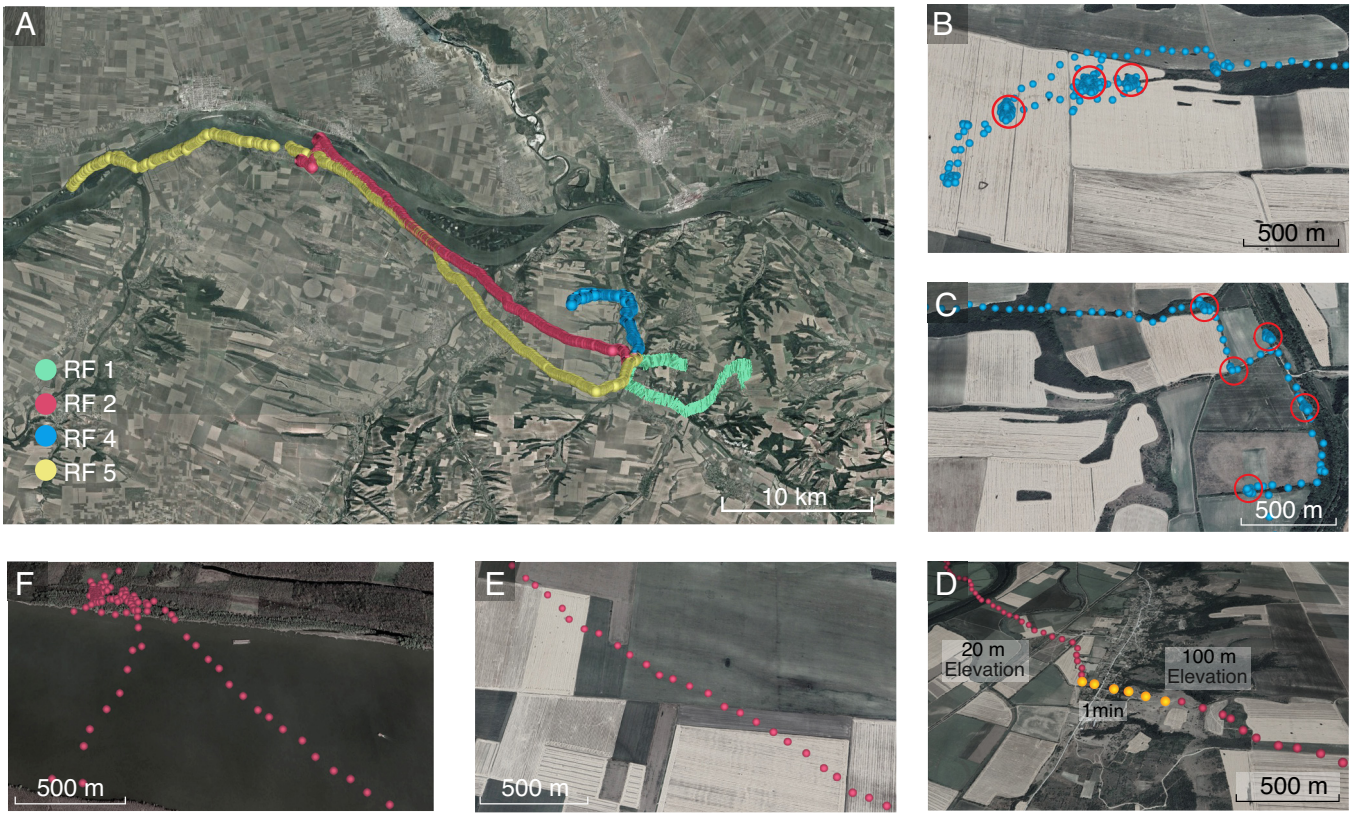

Fig. 2. Flight trajectories of four greater horseshoe bats. (*A*) Overview of the area with flight tracks of four individuals to their main foraging areas up to 40 km from the roost in RF 05 (yellow). (*B*) Main foraging area of RF 04 with perch hunting sites at vegetation islands around the poles of a high voltage power line crossing an open field depicted by red circles. (*C*) Flight track of RF 04 along the vertical contour of vegetation lines and short perching stops on the way out depicted by red circles. (*D*) Flight track of RF 02 including an ~80 s long flight over a cliff with no acoustic contact to the ground depicted by yellow points. (*E*) Flight track of RF 02 when flying about a horizontal contour-line of open fields. (*F*) The flight track of RF 02 when crossing the Danube and then perch-hunting at its main foraging area.

extends far to the side. At 40^0 the DS of 83% re 23^0 results in an overcompensation of only 17% (Fig. 4*C*).

The advantage of this DSC strategy is that it uncouples prey echoes from their angle-dependent DS in a large forward-directed and spatially limited sector. The carrier frequencies of insect body echoes are still close to $\mathbf{f_{max}}$ so that the upward pointing glints cover the clutter-free sensitive part of the auditory fovea. At larger bearing angles the fast reduction of the cosine results in a fast decrease of the DS re 23^0 to 0% at 90^0 which eliminates the advantage of DSC. These echoes returning from large bearing angles fall in a frequency range where the auditory threshold is distinctly higher and are thus attenuated, further reducing the risk of masking prey echoes (24).

The background echoes also revealed information about the type of vegetation the bats encountered. These echoes were characterized by multiple strong reflectors in the case of vertical vegetation background and were significantly more diffuse in the case of a horizontal field as we quantified based on their spectral SD ($P < 10^{-6}$, GLMM. Fig. 4*E* and compare the individual echoes in Fig. 4 *A* and *B*). In some cases, a salient vertical reflector (possibly a large stem) could be tracked in consecutive echoes as the bat passed by it, generating flow information (see yellow arrows in Fig. 4*A2*).

Flight without Spectral Acoustic Feedback. To apply DSC, bats need Doppler shifted environmental echo feedback, and this is probably why they nearly always maintained acoustic contact with the background. Based on the GPS data, we identified two situations in which bats flew without echo feedback that provides Doppler-information: 1) when bats flew over the Danube (Fig. 1*F*): when flying above mirror-like calm water all sound waves that hit the water with an aspect angle below or above 90° are reflected away from the bat (25). Only the weak reflection from the water surface directly below the bat is reflected. This echo (and especially its FM parts) allows the bat to estimate its altitude above the water, but it has a bearing angle of 90^0 and therefore no DS can be measured (Fig. 4*C1*). In a few events where we could detect these echoes, they indicated a flight height of about 1.2 m above water. 2) In a few situations the bats flew over a cliff and had no acoustic contact (26) with the ground for a short period (~1 min) before dropping and receiving echoes again (Figs. 1*D* and 4*C2*). In both echoless flight situations, the bats emitted echolocation signals that were 550 ± 50 Hz below their $\mathbf{f_{rest}}$ accounting for a partial DSC relative to their speed. While in the case of flying over water we could not be sure that the bats did not pick up weak echoes, e.g., from drifting objects or the shore that our microphone did not. In the second case however, the high altitude suggests that the bats had no access to any echoes. In both cases the response was the same, indicating that the bats had no acoustic feedback or the echoes were too weak to trigger DSC.

Modeling Doppler Shift Compensation. To model DSC, we fit GLMMs aimed to predict the next emission frequency (the explained variable) given the parameters of one or more of the previously received echoes. Based on the BIC parameter (*Materials and Methods*), the best explaining parameter in all bats was the DS of the maximal frequency ($\mathbf{f_{max}}$, Fig. 4*E* and *SI Appendix*, Table S1, i.e., the difference between the emitted frequency and the returning maximal frequency). Adding the frequency spread, the echo delay or the flight speed did not improve the models' fit. The model's fit improved when using multiple previous DS

as fixed factors with more recent echoes contributing more to the fit (Fig. 4*F*). Our modeling therefore suggests that bats integrate information from multiple previous echoes to control the emission of the next emitted call frequency. Notably, there was no difference between the models' parameters when fit to vertical and horizontal backgrounds, suggesting that the bats apply the same Doppler compensation strategy in both environments (compare red and blue lines in Fig. 4*F* and *SI Appendix*, Table S2).

Discussion

Filtering sensory inputs in a complex world is a fundamental challenge for all animal sensory systems. CF bats have evolved DSC to aid segregating prey from background which has been studied in the laboratory at many levels including behavioral, neurophysiological, and neuroanatomical studies (for a review see ref. 17). However, these studies could not address the main

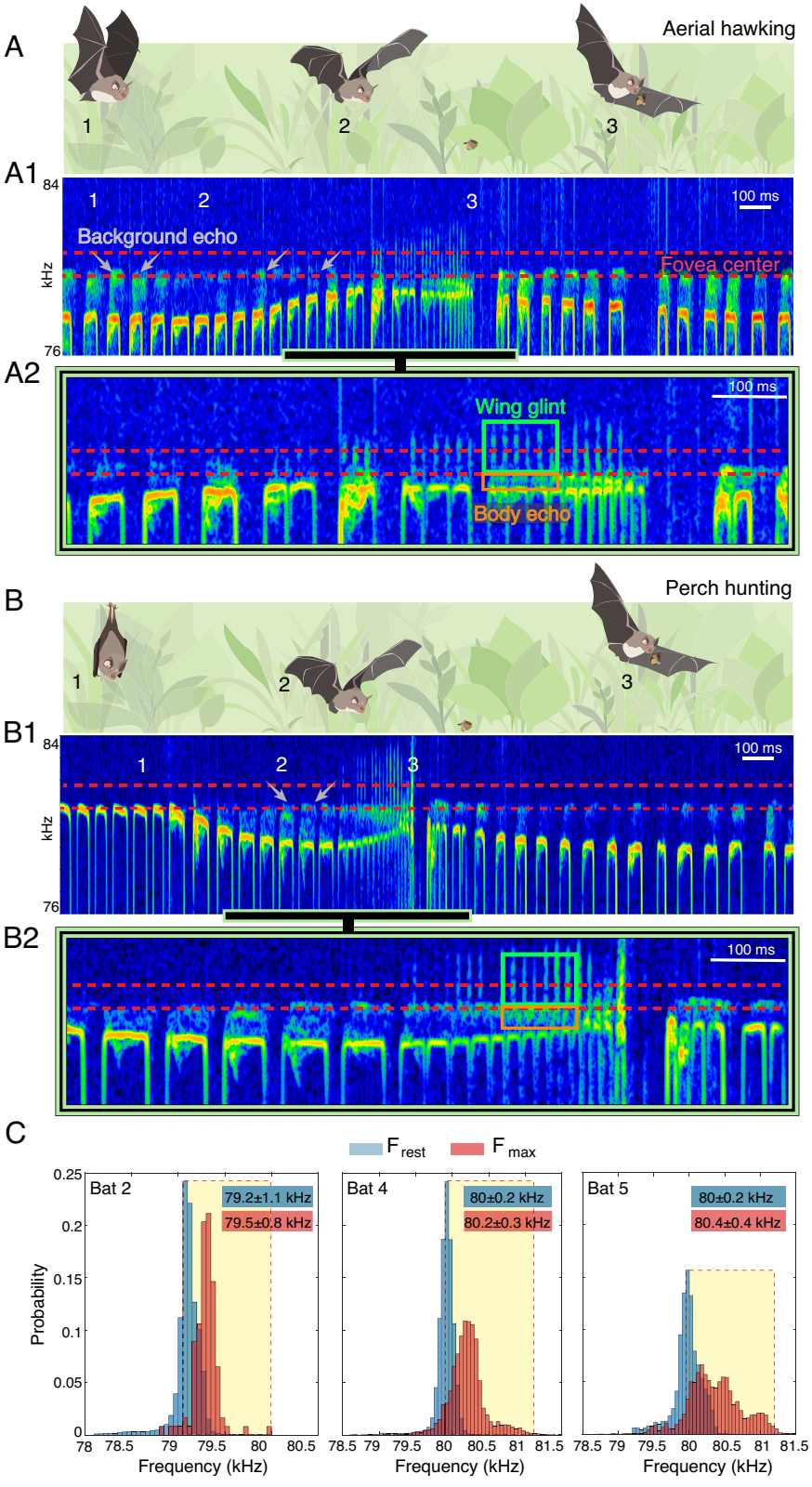

Fig. 3. Bats pursuing prey adjust their emission frequencies to receive upward prey echo-glints at the central auditory fovea. (*A*) An on-the-wing attack where a prey was detected by a commuting bat during continuous search flight along vegetation. The schematic depicts the stages of the attack corresponding to a 3 s long sound spectrogram (*A1*) with three behavioral phases: 1) search, 2) detection and 3) intercept. (*A2*) Zoom-in around the final moment of the attack. (*B*) A perch attack initiated by a bat that detected the prey while hanging at a perch. The schematic depicts three behavioral phases: 1) detection, 2) pursue and 3) intercept, corresponding to a 3 s long sound spectrogram (*B1*). (*B2*) Zoom-in around the final moment of the attack. All spectrograms are between 76-84 kHz. In both flight scenarios the maximum frequencies of the background echoes ($\mathbf{f_{max}}$) (see gray arrows *A1* and *B1*) are maintained just above $\mathbf{f_{rest}}$—indicated by the lower of the two red lines which delineate the 1 kHz wide most sensitive center area of the auditory fovea. The prey's echoes (green frame *A2* and *B2*) are characterized by a repeated series of up to 3.1 kHz wide upward wing glints riding on a visible carrier frequency ($\mathbf{f_{car}}$) below $\mathbf{f_{rest}}$ which is produced by the nonfluttering body of the prey (orange rectangle *A2* and *B2*). The glints cover the entire range of center of the auditory fovea. (*C*) The distributions of the resting frequencies ($\mathbf{f_{rest}}$—blue) and the maximum background echo frequencies ($\mathbf{f_{max}}$—red) for three of the bats (areas where the two distributions overlap appear in an intermediate color). The yellow rectangle depicts the most sensitive part of the auditory fovea.

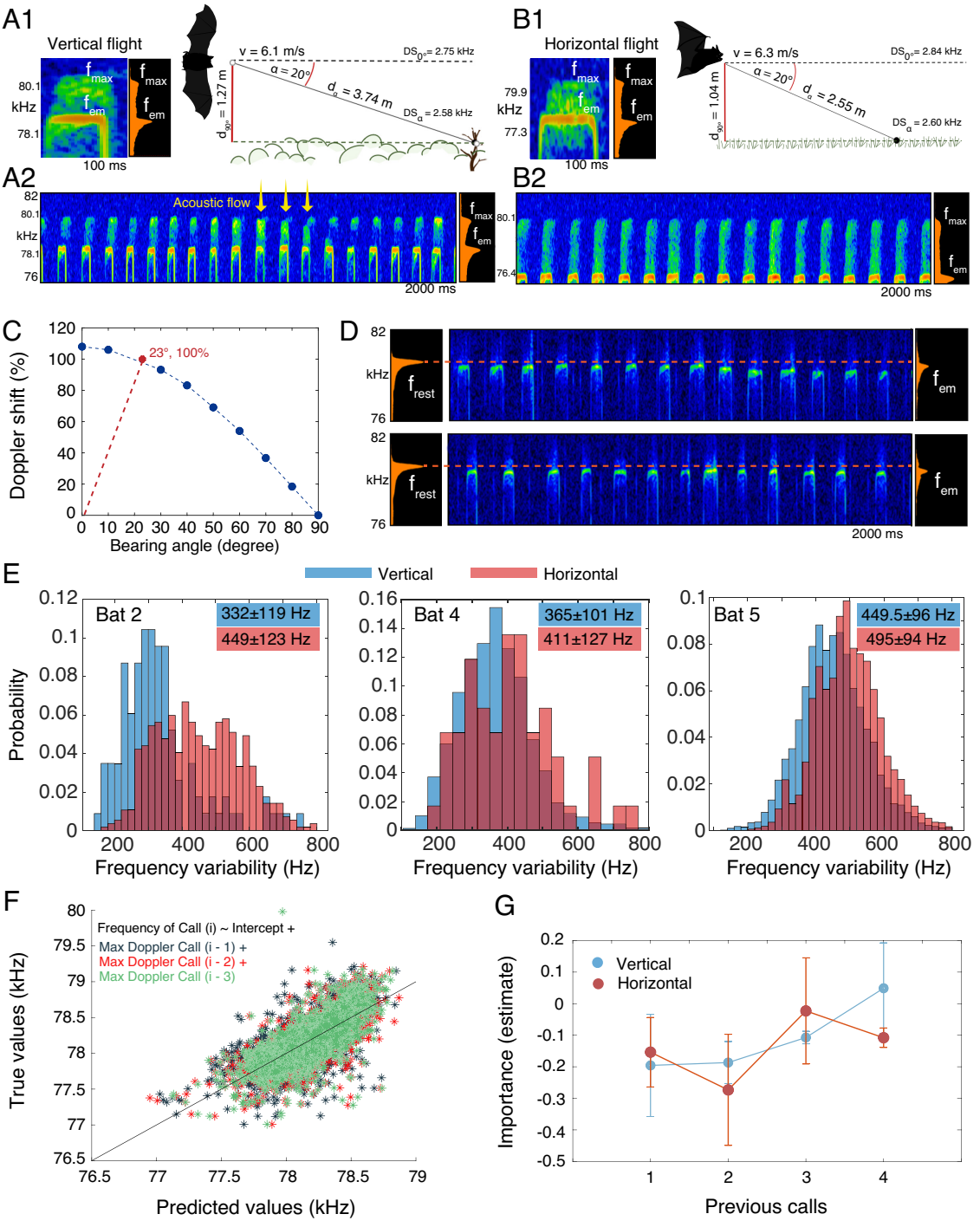

Fig. 4. Doppler shift compensation in bats flying along a vertical contour line and over a horizontal plane, and echolocation in bats flying without spectral acoustic feedback. For all spectrograms in this figure, the spectrum on the *Right* of the spectrogram shows an average of the adjacent signals. (*A* and *B*) *A1* and *B1* show schematics of typical echolocation scenes which have been used to determine the bearing angle. The relation between the highest measured DS and the maximal possible DS determined according to the bats' flight speed is equivalent to the cosine of the bearing angle between the direction to the effective target and the flight direction. The distance between the bat and the vegetation on the side can then be determined by the time delay between the emission and echoes with 0 Doppler-shift. In *A2* the bat flies beside a prominent reflector (yellow arrows) which appears at increasing bearing angles as the bat passes it (this could be for instance a prominent tree stem). This leads to decreasing DS with zero DS at 90° thus forming an acoustic flow field, i.e., a sequence of sounds that are nearing in time. When flying above horizontal background like a field or a meadow in *B2*, the relatively uniform targets reflect uniform echoes at all bearing angles and DS and generate diffusive echoes. In comparison, when flying near vertical background like a vegetation hedge in *A*, salient background echoes from directional reflectors can be seen. (*C*) The size of DS (in % re DS at 23^0) in prey echoes from different directions caused by the forward movement of a bat. Here, a DS compensation of 100% corresponds to a situation where $\mathbf{f_{max}}$ was adjusted to the echoes of an environmental target at 23^0. The size of bat flight-induced DS in echoes of insects with bearing angles between 0^0 and 23^0 is higher due to the higher speed vector of the forward moving bat. Below 23^0 the DS are smaller as the speed vector decreases with the cosine of the angle. (*D*) Spectrograms of bats crossing the Danube (*Upper*) or flying over a cliff (*Lower*) without echo-feedback in both cases. The emission frequency $\mathbf{f_{em}}$ in both situations was 550 ± 50 Hz below the resting frequency which is shown on the *Left* side for comparison. (*E*) Distributions of echo spectrum SD, used as a proxy of echo diffusivity demonstrate the difference between horizontal and vertical backgrounds. (*F*) Actual vs. model predicted emitted frequencies for one of the bats (RF 04). Results are shown for three of the best fit models when using the DS of the maximum frequency of one, two, or three previous calls. (*G*) Model estimates for the previous one to four calls suggest that the last previous call is most important for estimating, but that bats can use information even from three previous calls [mean ± SD for three bats are presented for vertical (blue) and horizontal (red) environments].

real-life challenges of whether horseshoe bats use DSC in the wild and, if so, how they perform it, which is what we examined in this study.

Greater Horseshoe Bats Receive Unmasked Prey Echo Glints at the Center of Their Acoustic Fovea. We analyzed the frequencies of the echolocation calls and echoes of vegetation and prey in free flying foraging greater horseshoe bats, and quantified the bearing angles and distances to vegetation targets. We show that the bats stayed in nearly permanent acoustic contact with the environment, allowing them to use DSC by lowering their emission frequency according to the incoming vegetation or ground echo information. This resulted in the highest frequencies in environmental echoes from targets with average bearing angles of up to ~23° and distances of ~4 m were maintained at a constant $\mathbf{f}_{max}$ of about 300 Hz above their $\mathbf{f}_{rest}$ (Figs. 3 and 4). As a result, DSC was most effective within a wide forward-directed and spatially limited sector in front of the bat (Fig. 4*C*).

These environmental echoes, essential not only for DSC but also for spatial orientation and environmental recognition, are received below $\mathbf{f}_{max}$, within the lower part of the central range of the fovea. In this frequency range, many specialized sharply tuned neurons are integrated into the audio-vocal control system for DSC (27–30) and possibly into the extraction of flow information for spatial orientation (31, 32). Indeed, by extracting the vegetation echoes, we show that the diffusivity of these highest frequency vegetation echoes provides information about the texture of the background distinguishing for example the uniform echo patterns of meadows (Fig. 4*A2*) from the more salient, structured echoes of trees or large stems (Fig. 4*B2*). This information could help to recognize landscape structures and together with the ranging information obtained by the FM component it can be used for spatial orientation or for identifying suitable foraging habitats.

Thanks to this DSC strategy applied by the bats, the echoes from the nonfluttering insect body ($\mathbf{f}_{car}$) were kept about 300 to 500 Hz below $\mathbf{f}_{rest}$, while the upward pointing broadband prey echo glints (up to 3.1 kHz) covered the clutter-free area of the central part of the auditory fovea above $\mathbf{f}_{max}$. In this frequency range, many sharply tuned, low threshold neurons are specialized for the detection and evaluation of flutter information (20, 21, 33). Thus, the bats received the prey's echo glints within the flutter sensitive center of the auditory fovea by sufficiently compensating for the DS induced by their own movement.

After compensating for the DS caused by the bat's flight, $\mathbf{f}_{car}$ and the glint direction of the prey depend only on the angular orientation and relative speed vector of the insect. Thus, by using DSC, the sensory task of flying bats searching for fluttering insects becomes similar to the task of a perching bat. The glints in all recorded insect echoes were upward in relation to $\mathbf{f}_{car}$ showing that the bats closed in on the insect from behind (at least at the end of the attack) where the backward moving insect wings cause upward DS in the instant of glint production (Fig. 1*D*).

The DSC strategy applied by the bats thus allows separating two behaviorally relevant information streams which are needed for spatial orientation on the one hand, and prey detection on the other. The strategy adjusts the two streams of information in the spectral domain so that they cover different frequency ranges (above and below $\mathbf{f}_{max}$) within the most sensitive central part of the auditory fovea. Our results reveal an active sensing strategy allowing to segregate signals from background input under natural conditions thus preventing interference and masking effects.

Greater Horseshoe Bats Control DSC Based on the $\mathbf{f}_{max}$ of Sufficiently Loud Background Echoes. Laboratory experiments have shown that in order to invoke the DSC response, the returning background echoes must be loud enough, have small interaural intensity differences (34), and overlap sufficiently with the emitted calls (35). Our results show that greater horseshoe bats used vegetation—and not prey—echoes to control their DSC. Indeed, background echoes that were maintained at $\mathbf{f}_{max}$ were loud, and their overlap with the echolocation calls were sufficient to elicit a DSC response (see spectrograms in Figs. 3 and 4). In contrast, prey echoes were very weak. This is in line with previous experiments showing that the bats do not lock in their DSC system on insect echoes and that the bats did not compensate for DS induced by the movement of the insects (36, 37) probably because the prey echoes were too weak to reach the activation threshold of the DSC system (34).

To identify which specific sensory features of the vegetation echoes bats might use to estimate their emission frequencies, we modeled the emitted frequency as a function of different background echo parameters. Our model suggests that freely flying bats in the wild might estimate the DS in relation to $\mathbf{f}_{max}$ and integrate information over at least 3 previous calls to adjust the emission frequency. This integration, which confirms former controlled laboratory experiments (38, 39) likely serves as a low-pass-filter, avoiding abrupt changes of the emission frequency in response to a single reflector. This is advantageous for tracking the vegetation contour, even when echo streams sometimes include discontinuities in depth structure, e.g., due to gaps in the vegetation. However, horseshoe bats with no acoustic contact with the environment while flying in the open or while receiving only a non-DS belly echo when flying over water surfaces adjusted the CF of their emitted signals to about 550 ± 50 Hz below $\mathbf{f}_{rest}$. At a flight speed of 5.5 m/s, which is typical for these bats based on our GPS assessments, prey echoes would be received in a frequency region not adapted for the detection of fluttering prey—above the auditory fovea. We hypothesize that adjusting the emission frequency below $\mathbf{f}_{rest}$ without acoustic feedback allows rapid detection of stationary background echoes (e.g., from vegetation or the ground) which will be received within the sensitive part of the auditory system, thus initiating subsequent tuning of the DSC via the bats' audio-vocal control system.

Our echo recordings are only a proxy of the sensory information available to real bats, because the bats likely have a more sensitive system and possess a directional pinna that filters the echoes differently from our microphone. Nevertheless the echoic scene we recorded is likely a good proxy of the available echoic information because: 1) our microphone is omnidirectional and thus picks up echoes returning from the bat's calls from all directions; 2) based on the greater horseshoe bat's hearing directionality (40), the lateral echoes with the low Doppler shifts picked up by our microphones were overemphasized in comparison to the real bat's reception, but this has no effect on our conclusions as we never used them in any relevant argument. 3) The forward directed echoes picked up by the tags may be somewhat attenuated in comparison to what real bats receive. This would result in slightly lower maximal detection ranges of our system, but we show that our system records echoes from up to 4 to 5 m, which have been shown to be the maximal relevant range for the DSC system (34, 35). 4) we moreover show that the echoes behave exactly as expected from hedge echoes in terms of their temporal-spectral shifts (e.g., see Fig. 4) and 5) we show a correlation between the GPS-based backgrounds (i.e., horizontal vs. vertical background) and the echoes (Fig. 4*A*). The bats might have received a slightly different echoic scene, but not a completely different one.

In conclusion, the DSC strategy applied by naturally foraging horseshoe bats gives rise to two information streams with different functions: 1) tracking the environment and 2) detecting prey. Thanks to this strategy, bats are not afflicted by background echo masking of the frequencies that are relevant for prey recognition. DSC allows horseshoe bats to find fluttering prey using their glint detection system in an environment which is highly cluttered but rich in prey along vegetation edges and above meadows. The situation where complex sensory inputs are received simultaneously by the brain and must be filtered to extract relevant information streams is common to all living organisms and all sensory modalities. Using a unique model organism, we demonstrate how this can be done already at the level of information acquisition.

Materials and Methods

Tagging. Greater horseshoe bats (*Rhinolophus ferrumequinum*) were caught at Nanin Kamak Cave, Bulgaria, during August 2018 and 2021 under permit numbers: 180/07.08.2018 and 891/ 26.07.2021 from MOEW-Sofia and RIOSV-Ruse. The bats were caught with hand nets during the day. We glued the tags to the fur on the back of the bats using Ostobond skin glue (Montreal Ostomy Products, Vaudreuil, Quebec, Canada) and released them back to their roost. The capturing, tagging, and releasing lasted approximately 30 min per bat. In total, we tagged 23 postlactating adult females (7 bats in 2018, 16 bats in 2021 with mean weights of: 23.5 ± 0.9 and 22.9 ± 0.8 g in 2018 and 2021 respectively).

In 2018, seven bats were tagged with Vesper tags (ASD, inc.) that weighed 3.9 g, thus accounting for 16.5% of the bats' body weight on average. The GPS was set to record position every 15 s. The extra weight was high, but the tagging duration was very short, as 2 d later we managed to retrieve five tags (of which one had malfunctioned). We and others have shown that such short tagging periods have minor effects on bats even with such high loadings (41–43). Audio data in 2018 were recorded using an ultrasonic Knowles (FG-23329, Knowles Electronics, Itasca, IL, US) microphone sampling at 200 kHz and with 12-bit resolution. In addition to GPS, the movement of the bats was recorded with triaxial accelerometers at a 50 Hz sampling rate and with a clipping level of 8 G. Most of the flight paths ended in the middle of the night when the batteries depleted, providing us with an average of 5 h of behavioral data per bat.

In 2021 the tags weighed 13% of the body weights of the tagged bats. Five tags were retrieved after up to 3 d later and weighing the bats before and after the tracking revealed that they lost on average 1.1 g of body weight. Audio was recorded with an ultrasonic Knowles microphone (FG-23329, Knowles Electronics, Itasca, IL, US) at a sampling rate of 187.5 kHz, with 16-bit resolution. Acceleration data were sampled at 1,000 Hz with a clipping level of 8 G. All accelerometer data were calibrated, converted into acceleration units (m/s^2) and decimated to 100 Hz. The recordings ended after an average of 5.5 h due to battery depletion. The bats returned to the colony on the same night they were tagged as we validated by checking the cave on the following day.

GPS Data Analysis. The GPS data allowed us to estimate the flight speed of the bats (average speed was estimated over four GPS locations 60 s apart). We further used the GPS data to (manually) detect segments when the bats were flying along vertical contours (i.e., woods or vegetation), horizontal contours (i.e., fields), and echoless environments (e.g., the Danube or over a cliff). To this end, the trajectory of the bats was examined (Fig. 2) and the background was classified according to the categories above (using Google earth). This method did not allow us to know the specific state of the fields while the bat was flying above them. For bats without GPS recordings, the acceleration data allowed us to distinguish between commute and perch hunting.

On-Board Microphone Characteristics. Most of the acoustic analysis was performed with the Vesper tags that also had a GPS and thus we perform a validation of microphone sensitivity and directionality of this device. The technical details of the second device were published before (44).

We performed two experiments to validate the Vesper microphone's directionality and sensitivity characteristics. For playback, we used a 78 kHz signal (50 ms long) whose intensity was measured with a calibrated GRAS 40DP 1/8-inch microphone (GRAS Sound & Vibration) so that the input signal's intensity was known in dB SPL re 1 m. All playbacks were performed with an ultrasonic dynamic Vifa speaker connected to UltraSoundGate 216H D/A converter (Avisoft Bioacoustics). 1) To characterize the directionality of the Vesper's microphone, we first played the signal at 94 dB SPL re 1 m, from 10 different directions ~36° apart on a 1 m circle around the sensor which was mounted horizontally–as if on the back of a flying bat. This analysis revealed a nearly omnidirectional response of the microphone (*SI Appendix*, Fig. S1). 2) Next, we measured the sensitivity of the Vesper's microphone by placing the speaker 1 m in front of the device (mounted as before) and played the signal at decreasing intensities (as was measured with the calibrated GRAS microphone), between 95 to 70 dB SPL re 1 m, at 5 dB steps. This analysis revealed that the noise floor of the microphone at this frequency is ~70 dB SPL.

Audio Data Analysis. We analyzed the echolocation calls and echoes of the three bats for which we had both audio and GPS data because only for these bats could we distinguish between flying along vertical and horizontal backgrounds and estimate flight speed. In total we analyzed 26,137 echolocation signals emitted in flight and 48,557 perching signals. We used the audio data from all tags to estimate the proportion of attacks performed from a perch or on-the-wing (the acceleration data could provide this information even without GPS).

All analyses were done in Matlab (the Mathworks Inc., Natick, Massachusetts, US).

Detection. Echolocation calls of flying bats were automatically detected as follows (*SI Appendix*, Fig. S2): The audio was first BP filtered around 80 kHz (± 10 kHz). The spectrograms were then transformed into a binary image based on a threshold set to the 97th percentile of the entire recording. The binary spectrogram was projected to the X-axis and smoothed with a moving window (of 1.3 ms) to generate an estimate of the envelope. Another threshold (92nd percentile) was then set to detect the beginning and end of the calls including their echoes when present. Thousands of calls were scrutinized manually in order to set these parameters before applying this procedure to all recordings.

Echo detection was next performed on the detected calls in the spectral domain. Calls with echoes were first detected based on having two distinct peaks in their spectrum using a peak detection function (Matlab, *SI Appendix*, Figs. S2 and S3). Next, the Doppler parameters of the echo (the second peak) were evaluated using a cross correlation of the echo's spectrum with that of the emitted signal. All spectral parameters were estimated on this signal. The time difference between these two peaks was defined as the ***echo's delay*** in the modeling part.

Echolocation parameter estimation (SI Appendix*, Fig. S2*). The frequency with maximum power in the signal's spectrum was defined as the emission frequency $\mathbf{f_{em}}$.

The echo's (maximum energy) frequency was computed by taking the peak of the cross correlation of the FFT magnitudes of the echo and the signal.

The maximal echo frequency ($\mathbf{f_{max}}$) was defined as the highest frequency at which the echo's FFT's magnitude was at least 20% of the global maximum of the echo's FFT.

The individual resting frequency ($\mathbf{f_{rest}}$) was computed by taking the average (per bat) of all perching echoes.

The echoes spectral SD (diffusivity) was estimated based on its SD: we computed the SD of echo energy across frequencies:

$\sigma_{echo} = \sqrt{\Sigma\left(f_n \cdot S_{echo}[n] - \frac{\Sigma f_n \bullet S_{echo}[n]}{N}\right)^2}$. Where: $S_{echo}[n]$ is the power spectrum of the echo and f_n is the corresponding frequency. The more diffuse the echo, the larger this measure will be.

Estimating the bearing angle (α). the angle ***a*** was estimated in two different methods–1) based on the bats' flight speed we could assess the proportion of the maximal Doppler shift that the bats compensated for. The relation between the actual measured highest DS and the maximal DS ahead is equivalent to the cosine of ***a***. This was done for 12 flight segments for the three bats with GPS data (six segments per bat). 2) We validated the first measurements by analyzing examples in which the 0 Doppler shifted echoes were visible which allowed us to assess the distance to side (or ground) vegetation. Together with the delay of the last returning echo (which was estimated based on the FM component that allows better time resolution; *SI Appendix*, Fig. S4), we could estimate the angle according to: Eq. 1 sine(***a***) = distance to the side/distance to farthest object.

Modeling. To model the DSC response, we fit GLMMs to each bat and each background separately (vertical–like high vegetation or horizontal–like fields). The explained parameter was the next emitted frequency while the fixed parameters (all defined above) that were tested were the Doppler shift of the echoes' maximal energy frequency and maximal frequency, the echo's spectral dispersion and the echo's time delay (i.e., the distance to the reflecting object). We also examined whether adding the bat's flight speed improved model fit. We used the speed sampled as close as possible in time to the calls, but our speed estimates were an average over many seconds which could explain why this parameter did not improve the models' fit. The BIC criterion was used to select the best fitting model. Once the best model was found (i.e., the Doppler of the maximal frequency), only this model was then tested with the echo parameters of multiple previous calls. We examined models with information from up to four previous calls (comparing them using the BIC). We note that the estimation of speed and echo delay were probably noisier: the speed was estimated based on GPS data, which was acquired once every 15 s only, and the delay was sometimes difficult to measure accurately.

Data, Materials, and Software Availability. Code and data have been deposited in Mendeley Data repository (10.17632/3vyvbrn9c9.1) https://data.mendeley.com/datasets/3vyvbrn9c9/1 (45).

ACKNOWLEDGMENTS. This research was supported by Villum Fonden grant no: 41386 (L.S.); and Israel Science Foundation grant no: 331/22 (Y.Y.).

Author affiliations: [a]School of Zoology, Faculty of Life Sciences, Tel Aviv University, Tel Aviv 6997801, Israel; [b]Sagol School of Neuroscience, Tel Aviv University, Tel Aviv 6997801, Israel; [c]Center for Active Sensing with Sound, Department of Biology, Aarhus University, Aarhus 8000, Denmark; [d]The School of Electrical Engineering, the Iby and Aladar Fleischman Faculty of Engineering, Tel Aviv University, Tel Aviv 6997801, Israel; [e]National Museum of Natural History Bulgarian Academy of Science, Sofia 1000, Bulgaria; and [f]Animal Physiology, Institute for Neurobiology, University of Tuebingen, Tuebingen 72076, Germany

1. A. de Cheveign, J. Z. Simon, Sensor noise suppression. *J. Neurosci. Methods* **168**, 195–202 (2008).
2. V. Padala, A. Basu, G. Orchard, A noise filtering algorithm for event-based asynchronous change detection image sensors on TrueNorth and its implementation on TrueNorth. *Front. Neurosci.* **12**, 1–14 (2018).
3. J. Engelmann, A. Wallach, L. Maler, Linking active sensing and spatial learning in weakly electric fish. *Curr. Opin. Neurobiol.* **71**, 1–10 (2021).
4. G. Maimon, A. D. Straw, M. H. Dickinson, Active flight increases the gain of visual motion processing in *Drosophila*. *Nat. Neurosci.* **13**, 393–399 (2010).
5. J. Najemnik, W. S. Geisler, Optimal eye movement strategies in visual search. *Nature* **434**, 387–391 (2005).
6. M. E. Nelson, M. A. MacIver, Sensory acquisition in active sensing systems. *J. Comp. Physiol. A Neuroethol. Sens. Neural. Behav. Physiol.* **192**, 573–586 (2006).
7. P. T. Madsen, M. Johnson, N. A. de Soto, W. M. X. Zimmer, P. Tyack, Biosonar performance of foraging beaked whales (*Mesoplodon densirostris*). *J. Exp. Biol.* **208**, 181–194 (2005).
8. L. Stidsholt *et al.*, Hunting bats adjust their echolocation to receive weak prey echoes for clutter reduction. *Sci. Adv.* **7**, 1–9 (2021).
9. J. A. Simmons, The resolution of target range by echolocating bats. *J. Acoust. Soc. Am.* **54**, 157–173 (1973).
10. B. Tian, H.-U. Schnitzler, Echolocation signals of the greater horseshoe bat (*Rhinolophus ferrumequinum*) in transfer flight and during landing. *J. Acoust. Soc. Am.* **101**, 2347–2364 (1997).
11. K. Fawcett, D. S. Jacobs, A. Surlykke, J. M. Ratcliffe, Echolocation in the bat, *Rhinolophus capensis*: The influence of clutter, conspecifics and prey on call design and intensity. *Biol. Open* **4**, 693–701 (2015).
12. N. Suga, M. Kawasaki, R. Burkard, Delay-tuned neurons in auditory cortex of mustached bat are not suited for processing directional information. *J. Neurophysiol.* **64**, 225–235 (1990).
13. R. Kober, H. Schnitzler, Information in sonar echoes of fluttering insects available for echolocating bats. *J. Acoust. Soc. Am.* **87**, 882–896 (1990).
14. H. U. Schnitzler, Die ultraschall-rrtungslaute der hufeisen-fledermäuse (Chiroptera-Rhinolophidae) in verschiedenen orientierungssituationen. *Z. Vergl. Physiol.* **57**, 376–408 (1968).
15. S. Hiryu, Y. Shiori, T. Hosokawa, H. Riquimaroux, Y. Watanabe, On-board telemetry of emitted sounds from free-flying bats: Compensation for velocity and distance stabilizes echo frequency and amplitude. *J. Comp. Physiol. A Neuroethol.* **194**, 841–851 (2008).
16. G. Neuweiler, G. Schuller, H.-U. Schnitzler, On- and off-responses in the inferior colliculus of the greater horseshoe bat to pure tones. *Z. Vergl. Physiol.* **74**, 57–63 (1971).
17. H.-U. Schnitzler, A. Denzinger, Auditory fovea and Doppler shift compensation: Adaptations for flutter detection in echolocating bats using CF-FM signals. *J. Comp. Physiol. A Neuroethol. Sens. Neural Behav. Physiol.* **197**, 541–559 (2011).
18. M. B. Fenton, P. A. Faure, J. M. Ratcliffe, Evolution of high duty cycle echolocation in bats. *J. Exp. Biol.* **215**, 2935–2944 (2012).
19. J. Ostwald, Tonotopical organization and pure tone response characteristics of single units in the auditory cortex of the Greater Horseshoe Bat. *J. Comp. Physiol. A Neuroethol. Sens. Neural. Behav. Physiol.* **155**, 821–834 (1984).
20. J. Ostwald, H. U. Schnitzler, G. Schuller, "Target discrimination and target classification in echolocating bats" in *Animal Sonar*, P. E. Nachtigall, P. W. B. Moore, Eds. (Plenum Press, ed. 156, 1988), pp. 413–434.
21. J. Ostwald, "Encoding of natural insect echoes and sinusoidally modulated stimuli by neurons in the auditory cortex of the greater horseshoe bat, Rhinolophus Ferrumequinum" in *Animal Sonar*, P. E. Nachtigall, P. W. B. Moore, Eds. (Springer, 1988), pp. 483–487.
22. H.-U. Schnitzler, "Echoes of fluttering insects: Information for echolocating bats" in *Recent Advances in the Study of Bats*, M. B. Fenton, P. A. Racey, J. M. V. Rayner, Eds. (Cambridge University Press, 1987), pp. 226–243.
23. G. von der Emde, H.-U. Schnitzler, Classification of insects by echolocating greater horseshoe bats. *J. Comp. Physiol. A.* **167**, 423–430 (1990).
24. G. R. Long, H. Schnitzler, Behavioural audiograms from the bat, Rhinolophus ferrumequinum. *J. Comparat. Physiol.* **100**, 211–219 (1975).
25. S. Greif, B. M. Siemers, Innate recognition of water bodies in echolocating bats. *Nat. Commun.* **1**, 107 (2010).
26. A. Boonman *et al.*, Echolocating bats can adjust sensory acquisition based on internal cues. *BMC Biol.* **18**, 1–10 (2020).
27. W. Metzner, A possible neuronal basis for Doppler-shift compensation in echolocating horseshoe bats. *Nature* **341**, 529–532 (1989).
28. W. Metzner, An audio-vocal interface in echolocating horseshoe bats.. *J. Neurosci.* **13**, 1899–1915 (1993).
29. W. Metzner, Anatomical basis for audio-vocal integration in echolocating horseshoe bats. *J. Comp. Neurol.* **368**, 252–269 (1996).
30. O. Behrend, G. Schuller, The central acoustic tract and audio-vocal coupling in the horseshoe bat, Rhinolophus rouxi. *Eur. J. Neurosci.* **12**, 4268–4280 (2000).
31. R. Müller, H. U. Schnitzler, Acoustic flow perception in cf-bats: Properties of the available cues. *J. Acoust. Soc. Am.* **105**, 2958–2966 (1999).
32. R. Müller, H. U. Schnitzler, Acoustic flow perception in cf-bats: Extraction of parameters. *J. Acoust. Soc. Am.* **108**, 1298–1307 (2000).
33. G. Schuller, Natural ultrasonic echoes from wing beating insects are encoded by collicular neurons in the CF-FM bat, *Rhinolophus ferrumequinum*. *J. Comp. Physiol. A. Neuroethol. Sens. Neural. Behav. Physiol.* **155**, 121–128 (1984).
34. O. Behrend, M. Kössl, G. Schuller, Binaural influences on Doppler shift compensation of the horseshoe bat *Rhinolophus rouxi*. *J. Comp. Physiol. A Neuroethol. Sens. Neural Behav. Physiol.* **185**, 529–538 (1999).
35. G. Schuller, Echo delay and overlap with emitted orientation sounds and Doppler-shift compensation in the bat, *Rhinolophus ferrumequinum*. *J. Comp. Physiol.* **114**, 103–114 (1977).
36. M. Trappe, H.-U. Schnitzler, Doppler-shift compensation in insect-catching horseshoe bats. *Naturwissenschaften* **69**, 193–194 (1982).
37. S. Mantani *et al.*, Echolocation behavior of the Japanese horseshoe bat in pursuit of fluttering prey. *J. Comp. Physiol. A Neuroethol. Sens. Neural Behav. Physiol.* **198**, 741–751 (2012).
38. G. Schuller, The role of overlap of echo with outgoing echolocation sound in the bat *Rhinolophus ferrumequinum*. *Naturwissenschaften* **61**, 171–172 (1974).
39. J. A. Simmons, Response of the Doppler echolocation system in the bat, *Rhinolophus ferrumequinum*. *J. Acoust. Soc. Am.* **56**, 672–682 (1974).
40. A. D. Grinnell, H. U. Schnitzler, Directional sensitivity of echolocation in the horseshoe bat, *Rhinolophus ferrumequinum*. *J. Comp. Physiol. A.* **116**, 63–76 (1977).
41. L. Stidsholt *et al.*, Echolocating bats prefer a high risk-high gain foraging strategy to increase prey profitability. *Elife* **12**, e84190 (2022).
42. K. Egert-berg *et al.*, Resource ephemerality drives social foraging in bats. *Curr. Biol.* **28**, 3667–3673 (2018).
43. M. Kelling *et al.*, Effects of tag mass on the physiology and behaviour of common noctule bats. *Mov. Ecol.* **12**, 38 (2024).
44. L. Stidsholt *et al.*, A 2.6-g sound and movement tag for studying the acoustic scene and kinematics of echolocating bats. *Methods Ecol. Evol.* **10**, 48–58 (2019).
45. L. Stidsholt, Y. Yovel, H.-U. Schnitzler, Data for: "Horseshoe bats foraging in the wild adjust sensing to separate prey echoes from background clutter." Mendeley Data, V1. https://data.mendeley.com/datasets/3vyvbrn9c9/1. Deposited 18 December 2025.